


Targeting pyroptosis reverses KIAA1199-mediated immunotherapy resistance in colorectal cancer

Lisha Li,¹ Lei Zhao,^{1,2,3} Diwei Zhou,⁴ Yuanhang Yu,¹ Peiyi Zhang,¹ Jingge Zheng,¹ Zhenyu Lin,^{1,2,3} Dandan Yu,^{1,2,3} Jinghua Ren,^{1,2,3} Jing Zhang,⁵ Pengfei Zhou,⁵ Dejun Zhang,^{1,2,3} Tao Zhang ^{1,2,3}

To cite: Li L, Zhao L, Zhou D, et al. Targeting pyroptosis reverses KIAA1199-mediated immunotherapy resistance in colorectal cancer. *Journal for ImmunoTherapy of Cancer* 2025;**13**:e010000. doi:10.1136/jitc-2024-010000

► Additional supplemental material is published online only. To view, please visit the journal online (<https://doi.org/10.1136/jitc-2024-010000>).

LL, LZ and DZ contributed equally.

LL, LZ and DZ are joint first authors.

Accepted 23 January 2025



© Author(s) (or their employer(s)) 2025. Re-use permitted under CC BY-NC. No commercial re-use. See rights and permissions. Published by BMJ Group.

For numbered affiliations see end of article.

Correspondence to
Professor Tao Zhang;
taozhangxh@hust.edu.cn

Professor Dejun Zhang;
zhangdejun@hust.edu.cn

ABSTRACT

Background Despite advancements in treatment modalities, several patients with colorectal cancer (CRC) remain unresponsive to immune checkpoint inhibitor therapy. Pyroptosis, an inflammatory programmed cell death process, holds substantial promise for tumor immunotherapy. In this study, we explored the use of pyroptosis to overcome immunotherapy resistance in CRC.

Methods We used a pyroptosis-related gene panel to construct an immunotherapy efficacy evaluation model and validated its performance by immunohistochemical staining of CRC patient samples. Pyroptosis and its underlying mechanisms were examined both in vitro and in vivo using PCR, western blotting, lactate dehydrogenase release assay, ELISA, co-immunoprecipitation, immunohistochemistry, fluorescence cell assays, microscopic imaging, flow cytometry analysis and bioinformatics approaches.

Results We established a model to define high or low levels of pyroptosis in CRC, revealed that low pyroptosis led to immunotherapy resistance, and identified KIAA1199 as a characteristic protein of low pyroptosis CRC. We further demonstrated that KIAA1199 contributes to low pyroptosis, resulting in resistance to immunotherapy. Mechanistically, KIAA1199 bound to and stabilized DNA methyltransferase-1 (DNMT1), thereby inhibiting GSDME-mediated pyroptosis. Importantly, our study highlighted that decitabine reversed KIAA1199-mediated immunotherapy resistance by enhancing pyroptosis to restore IL-1B release and CD8⁺ T cell infiltration.

Conclusions We found a critical role of KIAA1199 in promoting immunotherapy resistance by suppressing pyroptosis via the DNMT1/GSDME pathway in CRC. Decitabine has emerged as a promising therapeutic agent for reversing KIAA1199-mediated immunotherapy resistance by enhancing pyroptosis. Our findings provide valuable insights for enhancing the efficacy of immunotherapy in patients with CRC who exhibit resistance to conventional immunotherapy approaches.

BACKGROUND

Colorectal cancer (CRC) is the third most prevalent cancer globally and the second leading cause of cancer-related mortality.¹ Anti-programmed cell death-1 (PD-1) antibody has proven to be the first-line treatment

WHAT IS ALREADY KNOWN ON THIS TOPIC

⇒ Several patients with colorectal cancer (CRC) remain unresponsive to immune checkpoint inhibitor (ICI) therapy. Pyroptosis, an inflammatory programmed cell death process, holds substantial promise for enhancing tumor immunity. However, its potential and specific mechanism for overcoming immunotherapy resistance in CRC has not been fully explored.

WHAT THIS STUDY ADDS

⇒ KIAA1199 plays a critical role in promoting immunotherapy resistance by stabilizing DNMT1, which subsequently inhibits the expression and cleavage of GSDME and suppresses cell pyroptosis.

HOW THIS STUDY MIGHT AFFECT RESEARCH, PRACTICE OR POLICY

⇒ We explored the clinical significance of pyroptosis-related genes and KIAA1199 as potential biomarkers for predicting immunotherapy responses and proposed a novel treatment strategy combining decitabine with ICIs to reverse KIAA1199-mediated immunotherapy resistance by enhancing pyroptosis.

for CRC with deficient mismatch repair, which occurs in approximately 4%–5% of patients.^{2–5} However, it is imperative to acknowledge that other patients, do not demonstrate substantial clinical benefits of immune checkpoint inhibitors (ICIs).⁶ Anti-tumor immune escape is a critical factor contributing to immunotherapy resistance; however, the underlying mechanisms remain elusive. Thus, exploring the regulatory mechanisms of immune evasion in CRC and identifying effective inhibitory targets and clinical strategies are crucial. This effort is key to improving immunotherapy outcomes and CRC patient prognosis.

Pyroptosis, a well-studied form of programmed cell death (PCD), prominently implicates the gasdermin (GSDM) family that has been investigated across a spectrum of disease models, including autoimmune

and inflammatory diseases, infectious diseases, deafness, and cancer.^{7,8} Following cleavage, GSDM liberates the GSDM-N domain, which induces the piercing of the cell membrane. This process results in discernible morphological alterations, including cytoplasmic swelling, membrane rupture, and discharge of inflammatory factors into the extracellular environment.^{9,10} Thus, pyroptosis surpasses its role as a cellular endpoint. The induction of pyroptosis in tumor cells leads to the release of cytokines, including interleukin (IL)-1 β , IL-18, high mobility group box 1 protein (HMGB1), interferon-gamma (IFN- γ), granzyme (Gzm) -A/B/K, and Fas ligand (FasL).^{9,11} This process facilitates the recruitment of immune cells such as CD4⁺ T cells, CD8⁺ T cells, and natural killer (NK) cells into the tumor microenvironment, thereby orchestrating and amplifying the antitumor activity of the immune response. Wang *et al* have devised a bioorthogonal chemical system engineered to trigger GSDMA3-mediated pyroptosis in breast cancer cells. Pyroptosis-induced inflammation activates antitumor immunity and augments the therapeutic efficacy of anti-PD-1 treatment.¹² Another study introduced a bionic nanoparticle loaded with indocyanine green and decitabine specifically designed to trigger pyroptosis in tumor cells and enhance the sensitivity of immunotherapy for solid tumors.¹³ In conclusion, the inflammatory response elicited by pyroptosis can activate antitumor immunity and augment immunotherapy sensitivity. Consequently, the extent of pyroptosis in tumor cells may serve as a predictor of the antitumor immune response and effectiveness of immunotherapy.

KIAA1199 is also known as cell migration-inducing and hyaluronan-binding protein.^{14–20} Our previous research revealed increased expression levels of KIAA1199 in CRC tissues, correlating with invasion, metastasis, drug resistance, and poor prognosis in patients with CRC.^{21–24} Importantly, KIAA1199 acts as a pivotal suppressor in modulating the immune response and enabling CRC cells to evade immune surveillance.^{25,26} However, the molecular network underlying KIAA1199-mediated immunotherapy resistance in CRC remains poorly understood.

In this study, we investigated the involvement of pyroptosis in regulating the response to immunotherapy and the underlying mechanisms in patients with CRC. Mechanistically, KIAA1199 promoted resistance to immunotherapy by inhibiting pyroptosis via the DNA methyltransferase-1 (DNMT1)/GSDME pathway. Additionally, we explored the clinical significance of KIAA1199 as a target in immunotherapy resistance and proposed a new therapeutic strategy involving the combination of decitabine and ICIs to reverse KIAA1199-mediated immunotherapy resistance by enhancing pyroptosis.

METHODS

Cell culture and reagents

MC38 cells were obtained from the American Type Culture Collection (Rockville, Maryland, USA). Human CRC cells (HCT116, SW480, and LOVO) and CT26 cells were procured

from the Cell Bank, Type Culture Collection, Chinese Academy of Sciences (CBTCCAS, Shanghai, China). These cells were cultured in DMEM (HCT116, MC38) or RPMI 1640 (SW480, LOVO, CT26) (GIBCO, Grand Island, New York, USA), supplemented with 10% fetal bovine serum (BI, Israel), 50 μ g/mL gentamicin, 100 U/mL penicillin, and 0.1 mg/mL streptomycin. All human cell lines were authenticated using STR profiling within the last 3 years, and all experiments were performed with mycoplasma-free cells.

Patients, tissue samples, and gene chips analysis

Cancer tissue samples were obtained from patients with histopathologically confirmed CRC who were hospitalized at the Union Hospital, Tongji Medical College, Huazhong University of Science and Technology, from July 2020 to December 2022. None of the patients underwent adjuvant radiation treatment prior to surgery. The study protocol was thoroughly explained to the patients and written informed consent was obtained from each participant.

Immunohistochemistry

42 paraffin-embedded CRC specimens were obtained from the Union Hospital, Tongji Medical College, Huazhong University of Science and Technology. Tumor samples were sectioned into 4 μ m slices. Primary reactions were performed using anti-GSDMD, anti-caspase-1, anti-caspase-3, anti-NLRP3, anti-KIAA1199, anti-DNMT1, and anti-GSDME antibodies (Proteintech). This was followed by incubation with the secondary antibody and immunoperoxidase staining. The mean density of immunohistochemistry (IHC) staining was quantified using Image-Pro Plus 6.0, with scores of 0, 1, 2, and 3 assigned based on cell staining intensity and the percentage of positive cells. The scoring was based on the percentage of positive cells, classified into four levels: 1 point for 0% \leq positive cells \leq 25%, 2 points for 25% $<$ positive cells \leq 50%, 3 points for 50% $<$ positive cells \leq 75%, and 4 points for 75% $<$ positive cells \leq 100%. For analysis, scores of 2 and 3 were categorized as the high group, while scores of 0 and 1 were categorized as the low group. The results were confirmed independently by at least two pathologists.

Western blot analysis and pull-down assay

Proteins from cell lysates were separated using sodium dodecyl sulfate (SDS)-polyacrylamide gels and transferred onto nitrocellulose filter membranes. The membranes were then blocked in 5% nonfat milk for 1 hour and incubated with primary antibodies at 4°C overnight. The primary antibodies, including anti-GSDMD, anti-KIAA1199, anti-DNMT1, and anti- β -actin, were purchased from Proteintech (Rosemont, Illinois, USA), whereas the anti-GSDME antibody was purchased from Abcam (Cambridge, UK). Subsequently, the proteins were visualized using a western blot detection system (Bio-Rad, Hercules, California, USA) after treatment with horseradish peroxidase-conjugated secondary antibodies (Proteintech).

Cells transiently transfected with KIAA1199- Δ 1/ Δ 2/ Δ 3/ Δ 4/ Δ 5—myc, His-Ubiquitin, and DNMT1-Flag plasmids (GeneChem, Shanghai, China) were lysed according to

the protocol of the Immunoprecipitation Kit with Protein G Magnetic Beads (Beyotime, China). Subsequently, the lysate was incubated with myc, His, or Flag beads at 4°C overnight. Following incubation, the mixture was electrophoresed using SDS-PAGE for western blotting with anti-Myc, anti-His, and anti-Flag antibodies (Proteintech). All experiments were repeated at least three times.

Reverse transcription quantitative PCR

Total RNA was extracted from the cells using the TRIzol reagent (Invitrogen, Carlsbad, California, USA). Following reverse transcription, the mRNA levels of the following proteins were measured using the SYBR Green Real-time PCR Master Mix. All experiments were performed in triplicates.

The primers used in this assay were as follows: KIAA1199 forward: 5'-CACATTCCAACCTACCGGGCT-3', reverse: 5'-CCATTGTCAGCAAACCGGC-3'; DNMT1 forward: 5'-ACCGCTTCTACTTCTCGAGGCCTA-3', reverse: 5'-GTTGCAGTCCTCTGTGAACACTGTGG-3'; GSDME forward: 5'-CGTAGAGAGCCAGTCTTCATTT-3', reverse: 5'-AGCACAGGGTTTCTCAGATTTA-3'; and β -actin forward: 5'-ACCGAGCGTGGCTACAGCTTCACC-3', reverse: 5'-AGCACCCGTGGCCATCTCTTTCTCG-3'.

Microscopic imaging

The cells were evenly distributed into six-well plates at a density of 1.0×10^5 cells per well and subjected to specific treatments. Bright-field images were captured at 26°C by using a camera microscope (OLYMPUS IX71). All experiments were repeated at least three times.

Lactate dehydrogenase release assay

Cells were evenly seeded into 96-well plates at a density of 1.0×10^4 cells per well and treated with specific interventions. The assay solution was prepared according to the standardized procedure outlined in the kit instructions (CytoTox 96 cytotoxicity assay; Promega, Madison, Wisconsin, USA) and mixed with the cell supernatant or animal serum. The mixture was then incubated in the dark for 30 min. Optical density values were then measured at 450 nm. Each sample was assessed thrice to determine the actual lactate dehydrogenase (LDH) release. All experiments were performed at least three times.

ELISA

Following treatment, the concentrations of IL-1 β and IL-18 in cell culture supernatants and serum were assessed as per the manufacturer's instructions (Wuhan USC Scientific Company, Wuhan, China). Standard curves were generated using the purified cytokine standards provided in the kit. Each sample was analyzed at least three times and the average value was calculated to determine the actual concentration. All experiments were performed at least three times.

Flow cytometry analysis

The Annexin V-FITC Apoptosis Detection Kit (Beyotime) was used for pyroptosis analysis. Following specific treatments, the cells were harvested and incubated for 20 min at

room temperature in the dark, followed by flow cytometry (BD Accuri C6).

For flow cytometry analysis of tumor tissue, animal tumor tissue samples were minced and incubated in RPMI 1640 containing 1 mg/mL collagenase V, 0.5 mg/mL hyaluronidase, and 100 μ g/mL DNase I on a shaking table at 37°C for 50 min. Following red blood cell lysis, the cells were blocked with anti-mouse CD16/CD32 (TruStain-FcX, Clone 93, BioLegend, San Diego, California, USA) and subsequently incubated with the following antibodies: PerCP-Cy5.5-CD45 (BioLegend), BV785-CD3 (BioLegend), BV510-CD8 (BioLegend), PE-GZMB (Invitrogen), PE-Cy7-IFN- γ (BioLegend), and FITC-perforin (BioLegend). Finally, cells were fixed and analyzed using a flow cytometer (CytoFLEX LX). All data were analyzed using FlowJo software (TreeStar, Ashland, Oregon, USA).

Animal experiments

Stable mouse colon cancer cell lines, CT26 and MC38 overexpressing KIAA1199 or knockdown-KIAA1199 were established. Female BALB/c or C57BL/6 mice (aged 4–6 weeks) were randomly divided into four or six groups and tumor cells were subsequently injected subcutaneously. Female BALB/c nude mice (aged 4–6 weeks) were randomly assigned to four groups and subcutaneously injected with HCT116 colon cancer cells for experiments involving the KIAA1199 antibody. The InVivoMab anti-mouse PD-1 (CD279) antibody used in our study was from BioXcell, item number BE0146-100MG. Each mouse received an intraperitoneal injection of 200 μ g every 3 days. Tumor volume was monitored twice a week, and the mice were euthanized after 21 days. Tumor tissues and blood samples were collected for subsequent analyses.

Bioinformatics analysis

We established a database containing 80 pyroptosis-associated genes. Using the CRC dataset from the TCGA database (<https://portal.gdc.cancer.gov/>), we employed the single-sample gene set enrichment analysis (ssGSEA) algorithm of the R package “GSVA” to assess and quantify the pyroptosis level of each patient sample. The samples were subsequently stratified, with one-third of the samples exhibiting high pyroptosis levels designated as the high-pyroptosis group and one-third of the samples with low pyroptosis levels categorized as the low-pyroptosis group. Subsequent differential analysis was performed to identify genes associated with pyroptosis.

Next, patients were stratified into high-expression and low-expression groups based on the median immunohistochemical expression level of KIAA1199. Clinical data were collected, and Kaplan-Meier survival curves and forest plots for univariate Cox analysis of KIAA1199 were generated using the “Survival,” “survminer,” and “forestplot” R packages. From TCGA database (<https://portal.gdc.cancer.gov/>), we assessed the expression levels of KIAA1199 across 33 types of tumors. Additionally, we used the GEPIA online database (<http://gepia2.cancer-pku.cn/>) and the TIMER

2.0 database²⁷ (<http://timer.comp-genomics.org/>) to analyze gene-related information. Metagenetic methods were employed to estimate the cellular composition of the immune infiltrates. ssGSEA was used to evaluate immune cell types across 28 immune cell subpopulations.²⁸ Immunophenolic nuclides (IPS) from patients with CRC were retrieved from the Cancer Immunome Atlas (<https://tcia.at/home>) to assess their response to immunotherapy. The response score is the most comprehensive indicator of tumor immunogenicity, calculated by integrating four key determinants: effector cells, checkpoints/immunoregulators, antigen processing, major histocompatibility complex molecules (such as HLA), and immunosuppressive cells. The IPS has shown excellent performance in predicting responses to anti-CTLA4 and anti-PD1 immunotherapy.^{29,30} Furthermore, we used immune cell infiltration assessment methods from TIMER 2.0 website to investigate differences in immune cell infiltration between high-risk and low-risk groups in CRC. Pearson's correlation analysis was performed to explore the relationship between the risk score and immune-infiltrating cells. Additionally, we employed the ESTIMATE method (<https://bioinformatics.mdanderson.org/estimate/disease.html>) using expression data to estimate stromal cells and immune cells in malignant tumor tissues and compared differences in the estimate score, immune score, and stromal score between the high and low KIAA1199 expression groups.

Statistics

The data are presented as the mean±SD of at least three independent experiments. Bioinformatics analysis was conducted using the R software (V.4.0.0; <https://www.r-project.org/>). Results were visualized using PRISM V.5.0 (GraphPad Software, San Diego, California, USA), and differences between two groups were analyzed using Student's t-test. For comparisons involving multiple groups, either one-way or two-way analysis of variance (ANOVA) was performed, with the one-way ANOVA used to assess statistical significance. Statistical significance was set at $p < 0.05$.

RESULTS

Low level of pyroptosis is associated with immunotherapy resistance in patients with CRC

Given that pyroptosis is a known predictor of antitumor immune response and immunotherapy sensitivity, and in the absence of a universally recognized pyroptosis-specific gene set, we curated our gene selection through a thorough review of relevant literature and online databases. This analysis was conducted using single-ssGSEA on datasets from TCGA-COAD (461 patients with CRC) and TCGA-COADREAD (172 patients with CRC) cohorts (online supplemental table 1). Based on this comprehensive review, we identified and selected the 80 genes most strongly associated with pyroptosis. Then, we employed the ssGSEA algorithm of the R package "GSVA" to assess and quantify the pyroptosis level of each patient sample. We defined the first one-third of the samples exhibiting a high pyroptosis level as high pyroptosis, whereas the

lowest one-third of the samples displaying a low pyroptosis level as low pyroptosis (online supplemental figure 1A). Notably, our observations revealed that in CRC with low levels of pyroptosis, immune cell infiltration, particularly that of CD8⁺ T cells, was significantly reduced compared with that in CRC with high levels of pyroptosis (figure 1A). Microsatellite instability-high (MSI-H) is increasingly being recognized as the most important biomarker for identifying patients likely to benefit from ICIs.³¹ Our investigation revealed that microsatellite-stable (MSS) CRC exhibited a lower level of pyroptosis than MSI-H CRC. Specifically, 69% of the CRC cases characterized by low pyroptosis were MSS, whereas only 29% of the CRC cases with high pyroptosis belonged to this category (figure 1B). Patients with CRC with low pyroptosis tended to exhibit a poorer response to anti-PD1, PD-L1, or PD-L2 immunotherapies (figure 1C).

To validate the clinical correlation between pyroptosis and immunotherapy sensitivity, we gathered data from relevant literature and online databases (GSEA and GeneCards). From the identified pyroptosis-related genes, we selected five key markers—GSDMD, caspase-1, caspase-3, NLRP3, and GSDME according to published research—for further investigation.^{32,33} These genes were chosen as the most significant pyroptosis-related markers based on their relevance and importance. We analyzed a cohort of 42 patients with CRC who received ICIs using IHC and immunofluorescence (IF) staining (online supplemental figure 1B). In agreement with the findings of the bioinformatics analysis, we observed that in low-level pyroptosis CRC, CD8⁺ T cell infiltration was reduced in comparison to that in high-level pyroptosis CRC (figure 1D). Our investigation revealed that MSS CRC exhibited lower expression levels of these five genes than MSI-H CRC (online supplemental figure 1C). Approximately 87% of the CRC cases characterized by low pyroptosis were MSS, whereas only 68% of the CRC cases with high pyroptosis fell into this category (figure 1E). Notably, patients in the high-pyroptosis group showed a significant improvement in survival (figure 1F,G). The disease control rate (DCR) was also higher in the high-pyroptosis group than in the low-pyroptosis group (figure 1H). Collectively, these results suggest that low level of pyroptosis is associated with immunotherapy resistance in patients with CRC.

KIAA1199 contributed to low pyroptosis

Given the differential response to immunotherapy between high-pyroptosis and low-pyroptosis CRC, we further explored differential gene expression. Notably, the expression level of KIAA1199 was significantly upregulated in CRC cells with low pyroptosis when comparing the differentially expressed genes (DEGs) between the low pyroptosis group and the high pyroptosis group (figure 2A). KIAA1199 has garnered significant interest due to its distinct expression patterns in tumors and its crucial biological functions. Consequently, our research team has conducted a series of studies focusing on KIAA1199^{22,24,25,34,35}, particularly in

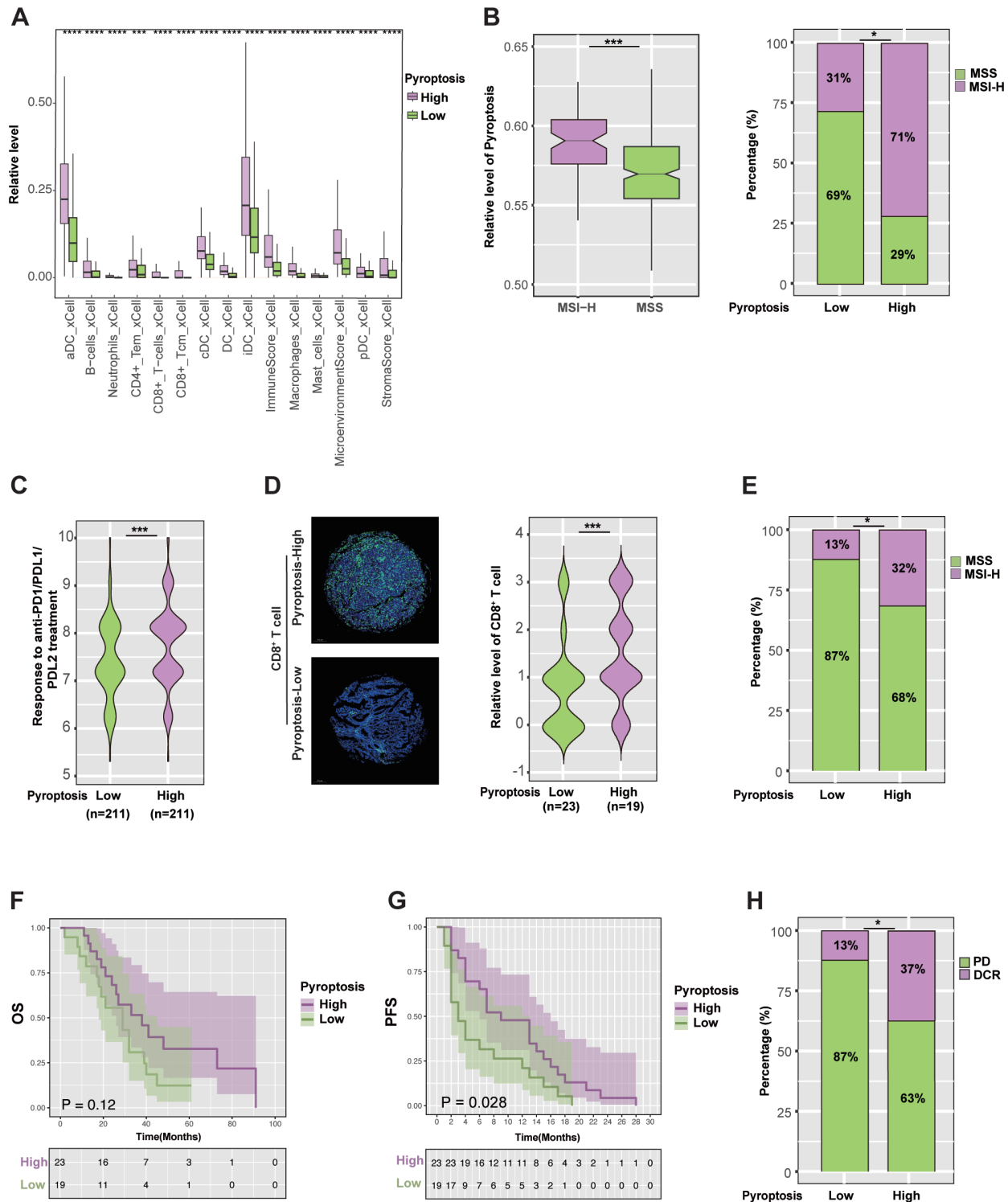


Figure 1 Low level of pyroptosis is associated with immunotherapy resistance in patients with CRC. (A) Comparison immune cell infiltration between patients with CRC (n=633). (B) Comparison of pyroptosis levels between patients with microsatellite instability-high (MSI-H) and microsatellite stable (MSS) CRC in tissues (n=633). (C) Comparison of responses to anti-PD1, PD-L1, or PD-L2 therapies between patients with CRC with high-level pyroptosis and those with low-level pyroptosis (n=633). (D) Comparison of CD8⁺ T cell infiltration between patients with CRC with high-level pyroptosis and those with low-level pyroptosis (n=42) through immunofluorescence (IF). (E) Comparison of MSI-H and MSS in high-level pyroptosis patients with CRC and low-level pyroptosis patients with CRC (n=42). (F) Comparison of overall survival (OS) between patients with CRC with high-level pyroptosis and those with low-level pyroptosis (n=42). (G) Comparison of progression-free survival (PFS) with immunotherapy between patients with CRC with high-level pyroptosis and those with low-level pyroptosis (n=42). (H) Comparison of the rate of disease control rate (DCR) and progression disease (PD) with immunotherapy between patients with CRC with high-level pyroptosis and those with low-level pyroptosis (n=42). Fisher's exact test was applied to B, E, and H. *p<0.05, ***p<0.001. CRC, colorectal cancer.

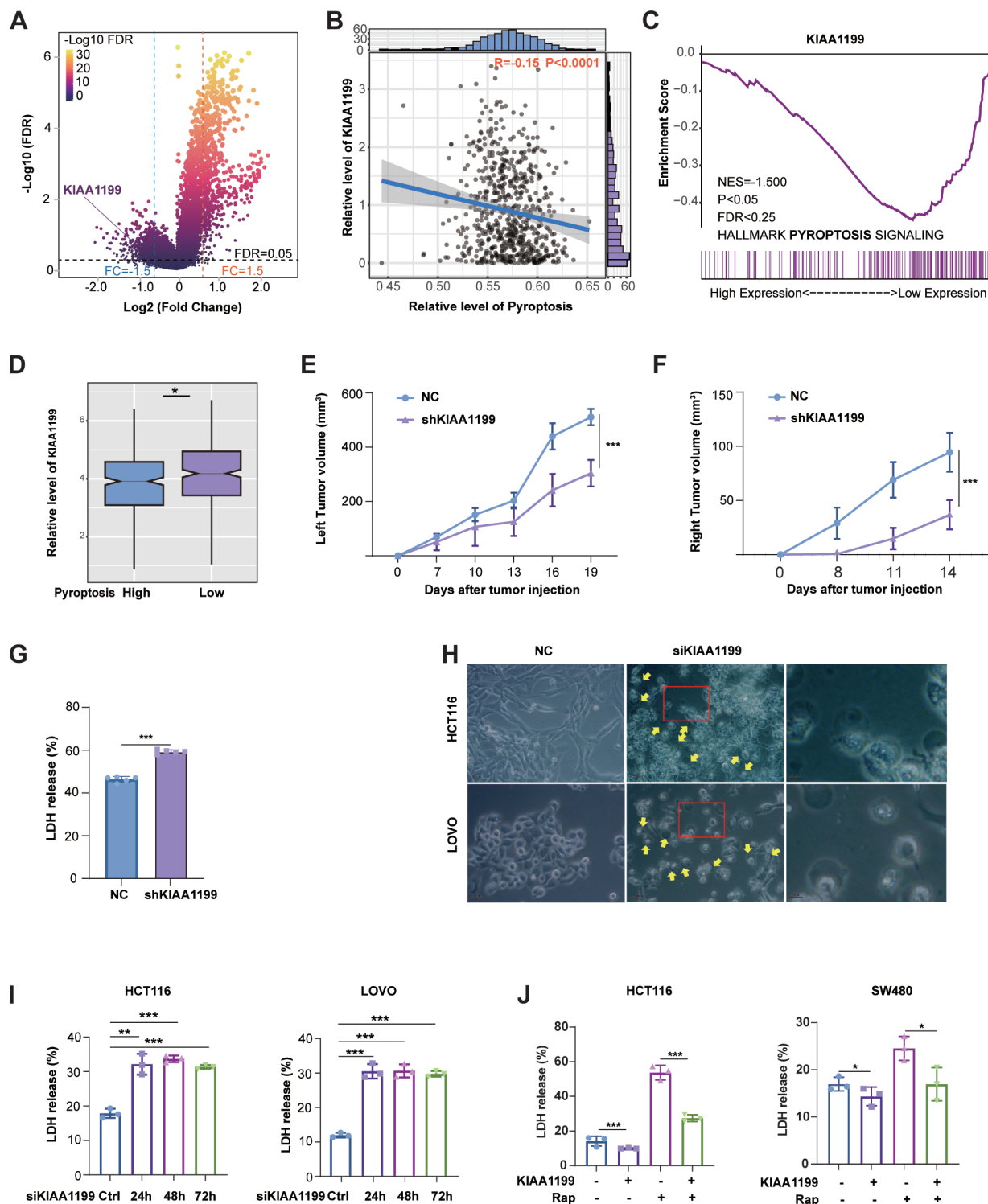


Figure 2 KIAA1199 is related to pyroptosis. (A) Further exploration of differential gene expression between patients with CRC with high-level pyroptosis and those with low-level pyroptosis (n=633). (B, C) Comparison of KIAA1199 expression levels between patients with CRC with high-level pyroptosis and those with low-level pyroptosis through Pearson correlation analysis (B) and Gene Set Enrichment Analysis (GSEA) (C). (D) Comparison of KIAA1199 expression levels between patients with CRC with high-level pyroptosis and those with low-level pyroptosis (n=633). (E) The tumor growth curves (left) of the NC and shKIAA1199 groups were plotted. (F) The tumor growth curves (right) of the NC and shKIAA1199 groups were plotted. (G) Lactate dehydrogenase (LDH) release of serum from NC and shKIAA1199 groups. (H) Images of HCT116 and LOVO cells treated with siRNA targeting KIAA1199 are shown. The scale bar represents 50 μm, and yellow arrowheads highlight the large bubbles emerging from the plasma membrane. (I) The release of LDH from the NC and siKIAA1199 groups of HCT116 and LOVO cells was measured. (J) The release of LDH from the NC and KIAA1199 groups of HCT116 and SW480 cells was measured. All experiments were repeated at least three times. * $p < 0.05$, ** $p < 0.01$, *** $p < 0.001$. CRC, colorectal cancer.

relation to immunotherapy resistance.²⁶ Pearson correlation and GSEA also revealed a close relationship between KIAA1199 and low pyroptosis (figure 2B–D). From the TCGA (<https://portal.gdc.cancer.gov/>) and GTEx database (<https://www.genome.gov/Funded-Programs-Projects/Genotype-Tissue-Expression—Project>), we observed a notable upregulation of KIAA1199 expression in various cancers, especially CRC (online supplemental figure 2A). Patients with low-KIAA1199 CRC demonstrated shortened disease-specific survival (online supplemental figure 2B). Moreover, we conducted IHC analysis of KIAA1199 in a cohort of 42 patients with CRC and observed significant upregulation in the expression level of KIAA1199 in low-pyroptosis CRC (online supplemental figure 2C and D).

There is widespread evidence that pyroptosis induces immunogenic cell death (ICD).⁷³⁶ To gain further insight into the relationship between KIAA1199 and pyroptosis, we employed a remote-effect model of ICD. BALB/c mice were initially injected with either NC- or shKIAA1199-CT26 on the left side. Five days later, all mice were injected with NC-CT26 on the right side (online supplemental figure 2E). Compared with the NC group, the shKIAA1199 group displayed a significant reduction in tumor growth on both the left and right sides (figure 2E,F, online supplemental figure 2E). Remarkably, only two out of five mice in the shKIAA1199 group developed tumors on the right side, the release of HMGB1 also indicating a spontaneous and substantial increase in ICD in shKIAA1199 tumors (online supplemental figure 2F). Subsequently, we found that the release of LDH into the serum was elevated in the shKIAA1199 group, providing evidence of pyroptosis (figure 2G). Moreover, KIAA1199 knockdown (KIAA1199-KD) resulted in pyroptotic cell morphology, characterized by large bubbles emerging from the plasma membrane, cell swelling (figure 2H, online supplemental figure 5H), and increased LDH release in a time-dependent manner (figure 2I, online supplemental figure 2G and H). To further verify the impact of KIAA1199 on pyroptosis, we used rapamycin (Rap), a rapid caspase-3 activator that triggers pyroptosis and is inhibited by KIAA1199 overexpression (KIAA1199-OE) (figure 2J, online supplemental figure 2H). In summary, our data strongly suggest that KIAA1199 inhibits pyroptosis.

KIAA1199 promoted immunotherapy resistance

Considering the association among KIAA1199, pyroptosis, and immunotherapy, we explored the effect of KIAA1199 on immunotherapy. We assessed immune cell infiltration in CRC using the TCGA database and the Timer2.0 web tool²⁷ (<http://timer.comp-genomics.org/>) and discovered a predominantly negative association between KIAA1199 and various immune cells, such as CD8⁺ T cells, CD4⁺ T cells, and NK cells (figure 3A, online supplemental figure 3A). KIAA1199 negatively correlated with ESTIMA and immune scores (online supplemental figure 3B and C). Furthermore, our analysis revealed that patients with MSS CRC had elevated expression levels

of KIAA1199 (online supplemental figure 3D). High-KIAA1199 CRC tended to exhibit a poorer response to anti-PD1, PD-L1, or PD-L2 therapies (online supplemental figure 3E). Furthermore, in a C57BL/6 mouse model, KIAA1199 facilitated the growth of subcutaneous tumors and suppressed sensitivity to anti-PD-1 immunotherapy (figure 3B, online supplemental figure 4A). Besides, anti-PD-1 treatment induced CD8⁺ T cell infiltration and IFN- γ ⁺ CD8⁺ T cells; however, it was inhibited by KIAA1199 (figure 2C,D, online supplemental figure 4B and C). Our previous study reached the conclusion when CRC cells with knockdown KIAA1199 were inoculated.²⁶

To further validate the clinical relevance of KIAA1199 expression, we analyzed a cohort of CRC tissues using IF staining and found that compared with low-KIAA1199 CRC, the infiltration of CD8⁺ T cells was decreased in high-KIAA1199 CRC (figure 3E). Furthermore, IHC analysis revealed that 97% of the high-KIAA1199 CRC cases were categorized as MSS (online supplemental figure 4D). Notably, higher KIAA1199 expression was associated with shorter survival and lower DCR (figure 3F–H). These results suggest that patients with high-KIAA1199 levels are resistant to immunotherapy.

KIAA1199 inhibited GSDME-mediated pyroptosis

The GSDM family is an effector mediating cell pyroptosis, except for DFNB59, which comprises both the C-terminal and N-terminal domains (GSDM-N).³² Currently, GSDMD and GSDME are recognized as key proteins that mediate pyroptosis; they are cleaved by caspase-1 and caspase-3, respectively, and release GSDM-N to pierce the cell membrane, inducing pyroptosis.³⁷ Our findings revealed that KIAA1199-KD resulted in the cleavage of GSDME with GSDME-N expression rather than GSDMD (figure 4A, online supplemental figure 5A and B). In the mouse model (online supplemental figure 2E), GSDME-N expression was dramatically elevated in KIAA1199-KD subcutaneous tumors (figure 4B). Moreover, GSDME is known to be cleaved by caspase 3.³² We used ac-DEVD-CHO (DEVD), a caspase-3 inhibitor, to hinder the cleavage of GSDME and observed that DEVD prevented GSDME-N expression induced by KIAA1199-KD (online supplemental figure 5D and E). GSDME knockdown (GSDME-KD) also produced a comparable effect (online supplemental figure 5F and G). We also employed Rap, a caspase-3 activator, to induce GSDME cleavage and found that Rap increased GSDME-N expression, which was suppressed by KIAA1199-OE (figure 4C, online supplemental figures 5C). This supports the hypothesis that KIAA1199 inhibited GSDME cleavage. Furthermore, treatment with DEVD to inhibit GSDME cleavage revealed that KIAA1199-KD upregulated both GSDME mRNA and protein expression in a time-dependent manner (online supplemental figure 6A and B). Additionally, we determined a negative correlation between the expression abundance of KIAA1199 and GSDME in human and mouse CRC cell lines; our results of clinical tumors also exhibited that (online supplemental figure

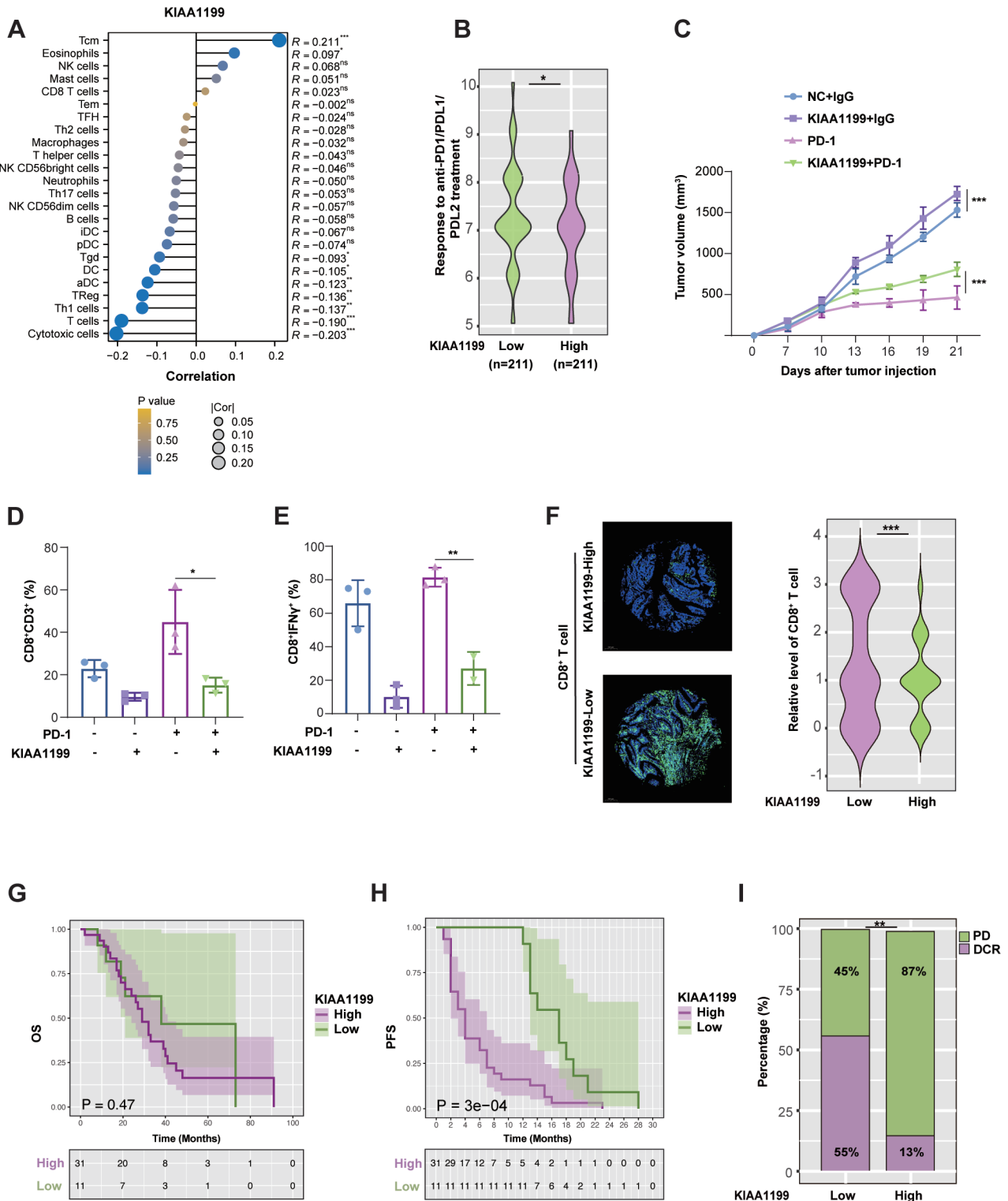


Figure 3 KIAA1199 could contribute to immunotherapy resistance. (A) KIAA1199 was compared with various significant immune cell subpopulations using data from the TCGA database. (B) Comparison of responses to anti-PD1, PD-L1, or PD-L2 therapies between patients with CRC with high-level KIAA1199 and those with low-level KIAA1199 (n=633). (C) The tumor growth curves of the NC and KIAA1199 groups with PD-1 were plotted. (D) The infiltration of CD 8⁺ T cells was analyzed by flow cytometry. (E) The infiltration of IFN-γ CD 8⁺ T cells was analyzed by flow cytometry. (F) Comparison of CD8⁺ T cell infiltration between patients with CRC with KIAA1199-high and those with KIAA1199-low (n=42) through IF. (G) Comparison of OS with immunotherapy between patients with CRC with KIAA1199-high and those with KIAA1199-low (n=42). (H) Comparison of PFS with immunotherapy between patients with CRC KIAA1199-high and those with KIAA1199-low (n=42). (I) Comparison of rate of PD and DCR with immunotherapy between patients with CRC with KIAA1199-high and those with KIAA1199-low (n=42). All experiments were repeated at least three times. Fisher's exact test was applied to panels H. *p<0.05, **p<0.01, ***p<0.001. CRC, colorectal cancer; IF, immunofluorescence; OS, overall survival; PFS, progression-free survival.

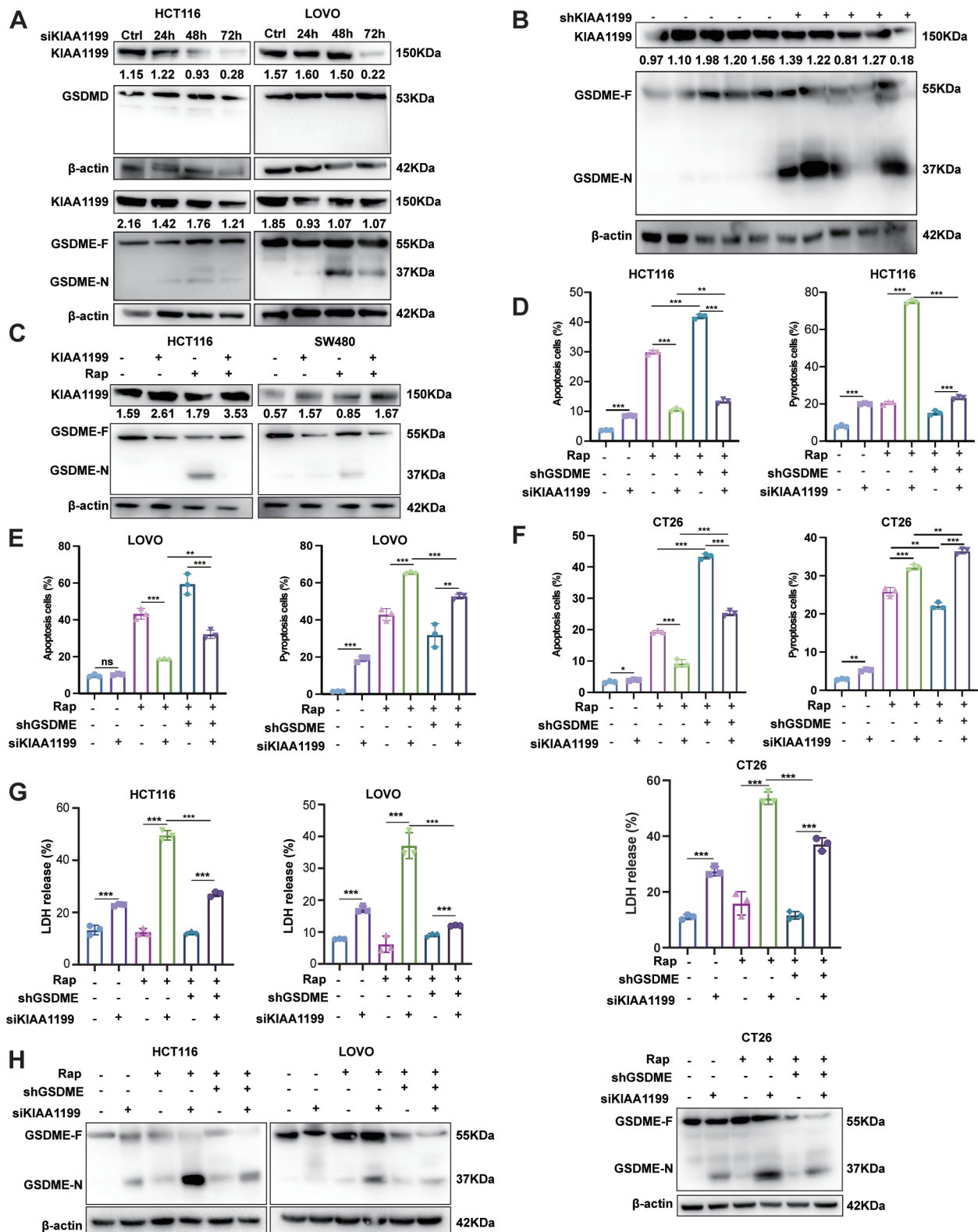


Figure 4 KIAA1199 converts GSDME-mediated pyroptosis to apoptosis in CRC. (A) Western blot analysis for GSDMD and GSDME expression. (B) Western blot analysis was performed to assess GSDME expression in xenografts from the NC and shKIAA1199 groups. (C) Comparison of GSDME-N expression levels in HCT116 and SW480 cells was measured. (D) The percentage of apoptosis and pyroptosis cells in HCT116 cells was analyzed by flow cytometry. (E) The percentage of apoptosis and pyroptosis cells in LOVO cells was analyzed by flow cytometry. (F) The percentage of Annexin V⁺ PI⁻ and Annexin V⁺ PI⁺ cells in CT26 cells was analyzed by flow cytometry. (G) Comparison of the release of LDH in HCT116, LOVO and CT26 cells was measured. (H) Comparison of GSDME-N expression levels in HCT116, LOVO and CT26 cells was measured. Western blot analysis was performed at least three times. β -actin was used as an internal control for normalization. All experiments were repeated at least three times. * p <0.05, ** p <0.01, *** p <0.001. CRC, colorectal cancer; LDH, lactate dehydrogenase.

6C–E). In summary, these data support the hypothesis that KIAA1199 inhibits GSDME expression, subsequently decreasing its cleavage.

To validate that KIAA1199 inhibited cell pyroptosis through GSDME, we examined the effect of GSDME on KIAA1199-inhibited pyroptosis. Our results showed that KIAA1199-KD or treatment with Rap increased the cleavage of GSDME and the release of LDH, especially combination of KIAA1199-KD and Rap remarkably did that. However, GSDME-KD aborted the cleavage of GSDME, and the release of LDH was upregulated by KIAA1199-KD and/or Rap (figure 4D–H, online supplemental figure 7A). Regarding the specific role of caspase-3 in regulating PCD, for example, apoptosis and pyroptosis, the expression level of GSDME influenced the conversion between apoptosis and pyroptosis. Notably, we observed that KIAA1199-KD increased pyroptosis and apoptosis when treated with Rap (a caspase-3 activator), KIAA1199-KD increased pyroptosis and decreased apoptosis, but these effects were reversed by GSDME-KD. Therefore, it provided evidence to suggest that KIAA1199 inhibited pyroptosis by suppressing GSDME-mediated conversion of apoptosis to pyroptosis.

Additionally, we developed antibodies (anti-KIAA1199) to bind and inhibit KIAA1199 (online supplemental figure 8A). The anti-KIAA1199 antibody effectively triggered GSDME-mediated pyroptosis (online supplemental figure 8B–G, online supplemental figure 9A). We verified these results in vivo (online supplemental figure 8H–J, online supplemental figure 9B and C). Our findings strongly suggested that KIAA1199 inhibited GSDME-mediated pyroptosis.

KIAA1199 inhibited GSDME by stabilizing DNMT1

To explore the underlying mechanism by which KIAA1199 inhibits GSDME, we conducted co-immunoprecipitation (Co-IP) and mass spectrometry (MS) peptide sequencing to identify KIAA1199-interacting proteins (online supplemental figure 10A). Our analysis revealed that DNA methyltransferase-1 (DNMT1) is a putative KIAA1199-interacting protein (online supplemental figure 10B). DNMT1 is a member of the DNMT family and comprises a conserved set of DNA-modifying enzymes that play central roles in epigenetic gene regulation.³⁸ To confirm the interaction between KIAA1199 and DNMT1, we performed co-IP experiments. Consistent with the MS results, we demonstrated an interaction between endogenous and exogenous KIAA1199 and DNMT1 (figure 5A,B, online supplemental figure 10C). To confirm the role of KIAA1199 in binding DNMT1, we constructed six KIAA1199 deletion variants tagged with C-terminal myc (online supplemental figure 10D). Then, pull-down assays revealed that KIAA1199-Δ4 (820–1204aa) was critical for binding DNMT1 (figure 5C). This indicates that KIAA1199 interacts with DNMT1.

To further investigate the influence of KIAA1199 on DNMT1, bioinformatics analysis and clinical tumors showed that KIAA1199 was positively correlated

with DNMT1 (online supplemental figure 10E–I). KIAA1199-KD resulted in a reduction in the protein level of DNMT1, whereas mRNA levels remained relatively unchanged. Conversely, KIAA1199-OE exerted the opposite effect by increasing the DNMT1 protein levels (online supplemental figure 10J–M). Moreover, treatment with cycloheximide (CHX) to inhibit protein synthesis showed that KIAA1199-OE extended the degradation time of DNMT1, whereas KIAA1199-KD shortened the degradation time of DNMT1 (figure 5D). Furthermore, compared with chloroquine (a lysosome inhibitor), only MG132 (a proteasome inhibitor) prevented the degradation of DNMT1 regulated by KIAA1199-KD (figure 5E). Importantly, ubiquitination assays showed that KIAA1199-KD led to increased ubiquitination of DNMT1 (figure 5F). This suggests that KIAA1199 upregulated the protein stabilization of DNMT1 by inhibiting ubiquitin and proteasome degradation.

Promoter methylation is an important reason for the low expression of GSDME in tumor tissues, thereby limiting the occurrence of pyroptosis.³² This methylation is intricately linked to the activity of DNMT family proteins.³⁹ Consistently, our bioinformatics and clinical tumor analyses revealed that DNMT1 was negatively correlated with GSDME and pyroptosis (online supplemental figure 11A and B). DNMT1-OE decreased both the protein and mRNA levels of GSDME (online supplemental figure 11C and D). Moreover, we found that KIAA1199-KD increased the expression and cleavage of GSDME and induced cell pyroptosis. However, this effect was suppressed by DNMT1-OE treatment (figure 5G, H, online supplemental figure 11E). This suggests that DNMT1 is essential to KIAA1199-inhibited pyroptosis. Collectively, these findings indicated that KIAA1199 stabilized DNMT1 and subsequently inhibited the expression and cleavage of GSDME and cell pyroptosis.

Decitabine reversed KIAA1199-mediated pyroptosis inhibition and immunotherapy resistance

Our findings proved that DNMT1 is essential to KIAA1199-inhibited pyroptosis and immunotherapy resistance. We used decitabine (DAC, a DNA methyltransferase inhibitor) to inhibit DNMT1 and found that DAC inhibited both the protein and mRNA levels of DNMT1 in a dose-dependent manner, leading to an increase in the expression and cleavage of GSDME (figure 6A and B), which is consistent with previous studies on breast cancer, melanoma, prostate cancer, and lung cancer.^{13 40–45} Moreover, we employed Rap (a caspase-3 activator) to induce pyroptosis and observed that KIAA1199-OE inhibited the Rap-induced expression and cleavage of GSDME (figure 6C, online supplemental figure 12A) and the release of LDH (figure 6D, online supplemental figure 12B); however, this effect was reversed by DAC treatment. This demonstrated that DAC could reverse KIAA1199-inhibited pyroptosis (figure 6E, online supplemental figure 12C–F).

Recently, targeting pyroptosis to activate antitumor immunity and sensitize patients to immunotherapy

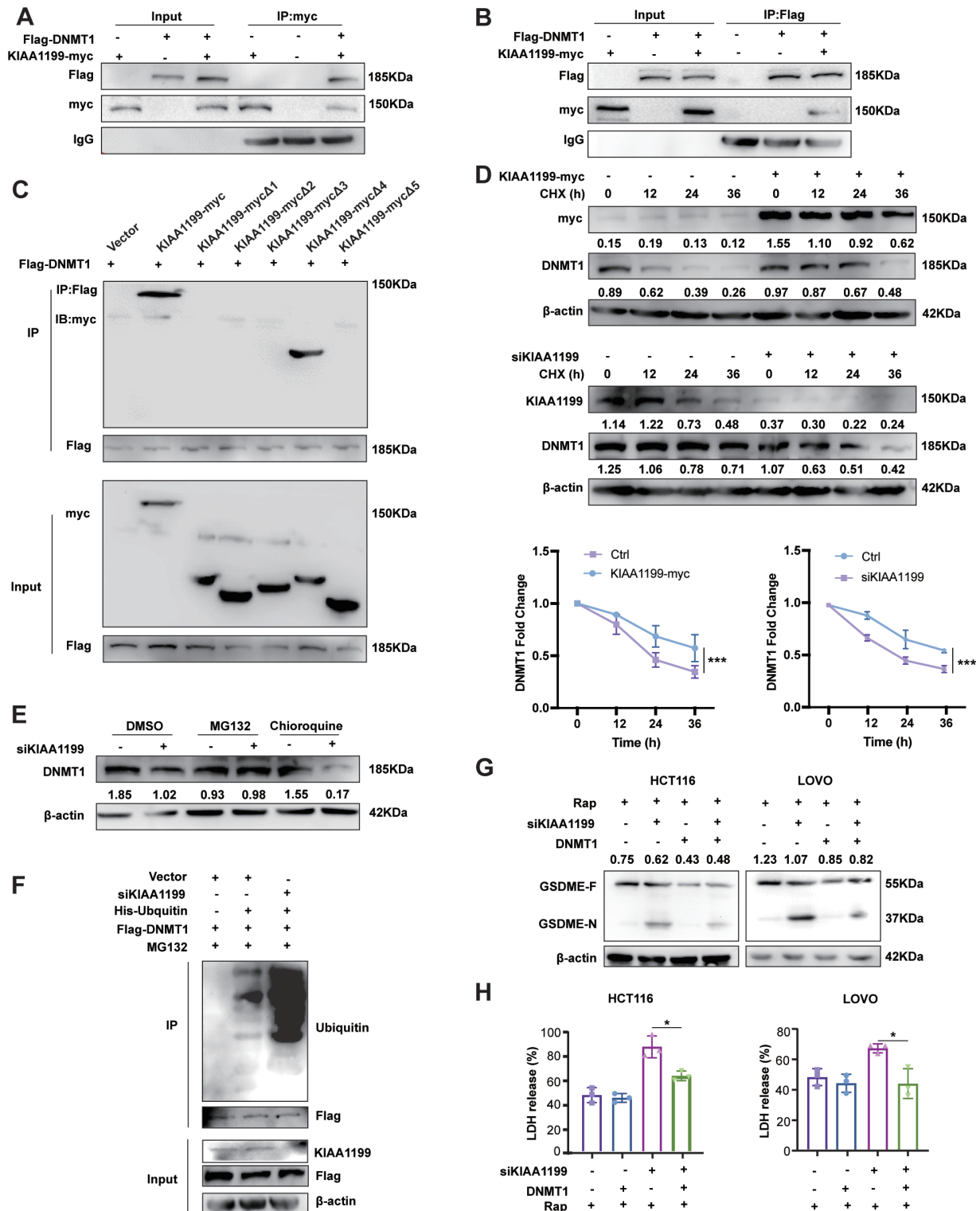


Figure 5 KIAA1199 inhibits pyroptosis by stabilizing DNMT1, thereby reducing the expression level of GSDME in CRC. (A, B) Co-IP experiments revealed a direct interaction between KIAA1199 and DNMT1. (C) Pull-down assays demonstrated that KIAA1199 deletion variants exhibited binding to DNMT1. (D) Comparison of DNMT1 and myc expression levels in HCT116 cells treated with cycloheximide (CHX) was measured (up). Protein bands were quantified using Image J (down). (E) Comparison of DNMT1 expression levels in HCT116 cells treated with DMSO, chloroquine, MG132 or siRNA of KIAA1199 was measured. (F) Ubiquitination assays revealed the relationship between KIAA1199 and the ubiquitination level of KIAA1199. (G) The expression levels of GSDME-N in HCT116 and LOVO cells were compared following treatment with raptinal, siRNA of KIAA1199, or overexpression of DNMT1. (H) LDH release in HCT116 and LOVO cells were compared following treatment with raptinal, siRNA of KIAA1199, or overexpression of DNMT1. Western blot analysis was performed at least three times. β -actin was used as an internal control for normalization. All experiments were repeated at least three times. * $p < 0.05$, *** $p < 0.001$. CO-IP, co-immunoprecipitation; CRC, colorectal cancer.

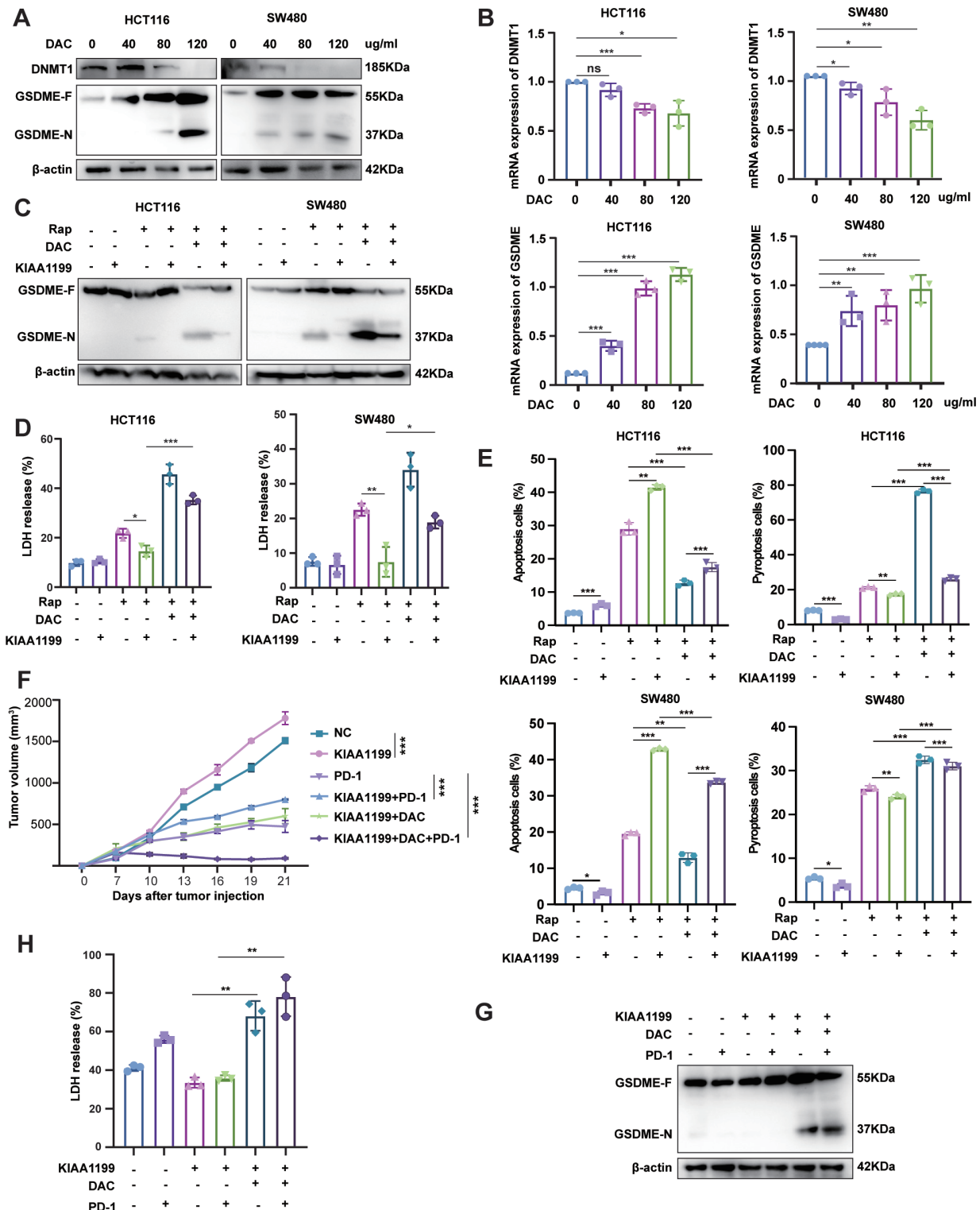


Figure 6 Decitabine reverses the inhibition of pyroptosis mediated by KIAA1199 and sensitizes immunotherapy. (A) Comparison of DNMT1 and GSDME expression levels in HCT116 and SW480 cells treated with decitabine was measured. (B) Comparison of DNMT1 and GSDME mRNA levels in HCT116 and SW480 cells treated with decitabine was measured. (C) The expression levels of GSDME in HCT116 and SW480 cells were compared following treatment with DAC, raptinal, and overexpression of KIAA1199. (D) LDH release in HCT116 and SW480 cells was compared following treatment with DAC, raptinal, and overexpression of KIAA1199. (E) The percentage of apoptosis and pyroptosis cells in HCT116 and SW480 cells following treatment with DAC, raptinal, and overexpression of KIAA1199 was analyzed by flow cytometry. (F) The tumor growth curves of the six groups were plotted. (G) Western blot analysis was performed to assess GSDME expression in xenografts from the six groups. (H) LDH release of serum from the six groups. Western blot analysis was performed at least three times. β -actin was used as an internal control for normalization. All experiments were repeated at least three times. * p <0.05, ** p <0.01, *** p <0.001.

has received increasing attention.^{9 10 12 46–48} Given that DAC aborts KIAA1199-inhibited pyroptosis by targeting DNMT1, we explored whether DAC could counteract KIAA1199-mediated resistance to immunotherapy. In the C57BL/6 mouse model, KIAA1199-OE resulted in anti-PD-1 inhibitor resistance, which was reversed by DAC treatment (figure 6F, online supplemental figure 12G). We investigated the reasons for this phenomenon. DAC increased GSDME cleavage in subcutaneous tumors and LDH levels in mouse serum (figure 6G,H). This indicated that DAC reversed KIAA1199-mediated immunotherapy resistance by inducing pyroptosis in vivo. In summary, these data suggested that DAC reversed KIAA1199-mediated immunotherapy resistance by augmenting pyroptosis. This offers a promising therapeutic approach for overcoming immunotherapy resistance in high-KIAA1199 or low-pyroptosis CRC.

Decitabine restored KIAA1199-suppressed CD8⁺ T cell infiltration by increasing IL-1 β release

It has become increasingly evident that pyroptosis has become a key focus of research owing to its capacity to reshape the tumor microenvironment by recruiting immune cells through the release of chemokines,^{12 46 49 50} such as IL-1 β and IL-18.^{11 51} We found that KIAA1199-KD increased the levels of IL-1 β and IL-18 in the presence or absence of Rap (figure 7A, online supplemental figure 13A). On the contrary, KIAA1199 inhibited the release of IL-1 β and IL-18, whereas DAC reversed this effect, particularly IL-1 β (figure 7B, online supplemental figure 13B). Moreover, we evaluated the level of IL-1 β in mouse serum and the infiltration of CD8⁺ T cells in subcutaneous tumors. Our results showed that KIAA1199-OE decreased the release of IL-1 β and the infiltration of CD8⁺ T cells with or without anti-PD-1 inhibitor treatment. Additionally, a combination of DAC and anti-PD-1 inhibitor dramatically augmented IL-1 β release and CD8⁺ T cell infiltration that were suppressed by KIAA1199, compared with either anti-PD-1 inhibitor or DAC alone (figure 7C, D, online supplemental figure 14A and B). This suggested that DAC restored KIAA1199-suppressed IL-1 β release and CD8⁺ T cell infiltration.

To elucidate the influence of IL-1 β on KIAA1199-suppressed CD8⁺ T cell infiltration, we employed anti-IL-1 β to block IL-1 β , and anti-CD8 to eliminate CD8⁺ T cells (online supplemental figure 15A). KIAA1199-KD suppressed the growth of xenograft tumors, which was reversed by anti-IL-1 β or anti-CD8, particularly anti-CD8 (figure 7E, online supplemental figure 15B). Consistent with our previous findings, KIAA1199-KD increased LDH levels in the mouse serum and GSDME cleavage in subcutaneous tumors. However, anti-IL-1 β and anti-CD8 had no influence on cell pyroptosis (figure 7F,G, online supplemental figure 15E). This suggests that IL-1 β and CD8⁺ T cells might be downstream of KIAA1199-inhibited pyroptosis. Moreover, we observed that KIAA1199-KD increased the release of IL-1 β and the infiltration of CD8⁺ T cell, and anti-CD8 did not affect the release of

IL-1 β , but anti-IL-1 β diminished the increase of CD8⁺ T cells (figure 7H,I, online supplemental figure 15C and D). This supported that KIAA1199-KD resulted in cell pyroptosis and IL-1 β release by recruiting CD8⁺ T cells. In conclusion, our results demonstrated that DAC restored KIAA1199-suppressed CD8⁺ T cell infiltration by enhancing pyroptosis-released IL-1 β .

DISCUSSION

In this study, we established a model to define high or low levels of pyroptosis in CRC and revealed that low pyroptosis led to immunotherapy resistance and identified KIAA1199 as a characteristic protein of low pyroptosis CRC. We further demonstrated that KIAA1199 contributes to low pyroptosis, resulting in resistance to immunotherapy. Mechanistically, KIAA1199 bound to and stabilized DNMT1, thereby inhibiting GSDME-mediated pyroptosis. Importantly, our study highlighted that decitabine reversed KIAA1199-mediated immunotherapy resistance by enhancing pyroptosis to restore IL-1 β release and CD8⁺ T cell infiltration.

Numerous investigations have demonstrated that pyroptosis possesses the ability to recruit immune cells, thereby transforming “cold” tumors into “hot” tumors through the release of cytokines and is widely acknowledged to induce ICD.^{9 36 44} Given the pivotal role of pyroptosis in eliciting tumor immunity, models based on pyroptosis-related genes have emerged to predict patient prognosis and assess the efficacy of immunotherapy in various solid tumors, including lung cancer, bladder cancer, glioma, kidney cancer, and histiosarcomas.^{52–56} In this study, we developed a model to predict clinical outcomes and immunotherapy responses among patients with CRC, thereby advancing the field of precision medicine. Interestingly, patients were ranked from highest to lowest according to their levels of pyroptosis. Using the median as a cut-off to distinguish between high and low pyroptosis groups could introduce minimal differences between patients near the threshold. To address this, we excluded patients with median pyroptosis levels, following the approach of several highly cited studies,⁵⁷ and used the top and bottom thirds as cut-off values for comparison. This approach demonstrated that the association between low levels of pyroptosis and immunotherapy resistance in patients with CRC is robust within this range. Notably, the stricter the cut-off, the stronger the observed effect.

Based on our previous studies, KIAA1199 has emerged as a pivotal suppressor gene implicated in the modulation of immune responses, enabling CRC cells to evade immune surveillance.^{25 26} Here, we show that KIAA1199 contributes to immunotherapy resistance by inhibiting pyroptosis. Research has shed light on the intricate interplay between signaling pathways governing apoptosis and pyroptosis.³² Our findings underscore the significance of KIAA1199 as a pivotal switch capable of converting low immunogenic apoptosis into highly immunogenic pyroptosis. This highlights KIAA1199 as a promising clinical molecular target for CRC treatment, with the potential to induce ICD by orchestrating the transition

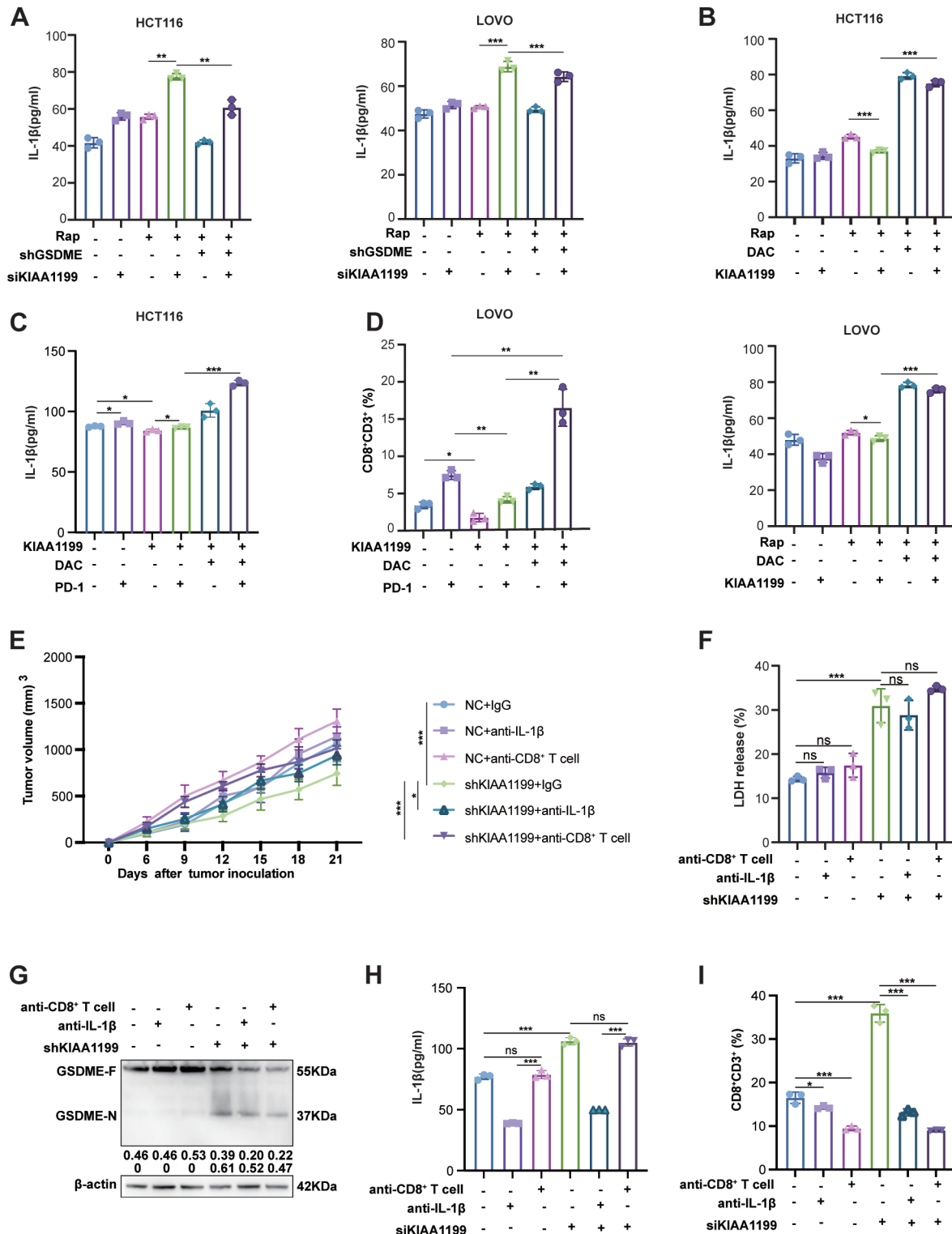


Figure 7 Decitabine restores the release of IL-1β and the infiltration of CD8⁺ T cells suppressed by KIAA1199. (A) IL-1β release was compared in HCT116 and LOVO cells treated with DAC, rapitinal, and siRNA of KIAA1199 in tumor culture supernatants. (B) IL-1β release was compared in HCT116 and LOVO cells treated with DAC, rapitinal, and overexpression of KIAA1199 in tumor culture supernatants. (C) IL-1β release of serum was analyzed by ELISA. (D) The infiltration of CD8⁺ T cells was analyzed by flow cytometry. (E) The tumor growth curves of the six groups were plotted. (F) LDH release of serum from the six groups. (G) Western blot analysis was performed to assess GSDME expression in xenografts from the six groups. (H) IL-1β release of serum was analyzed by ELISA. (I) The infiltration of CD8⁺ T cells was analyzed by flow cytometry. All experiments were repeated at least three times. **p*<0.05, ***p*<0.01, ****p*<0.001. LDH, lactate dehydrogenase.

between apoptosis and pyroptosis. Given its pivotal role, the development of a KIAA1199 antibody represents a critical advancement, laying a solid foundation for the clinical translation and application of KIAA1199 as a therapeutic target.

Previous studies have indicated that GSDME is frequently subjected to epigenetic silencing through methylation in a significant proportion of primary gastric tumors and colorectal adenocarcinomas, shedding light on the critical mechanism that contributes to the suppression of GSDME expression in tumor tissues.^{58 59} Our research revealed a potential mechanism whereby KIAA1199 inhibits the ubiquitination and degradation of DNMT1 in CRC by binding to DNMT1, leading to the methylation of GSDME and ultimately repressing GSDME expression. DAC received FDA approval for the treatment of myelodysplastic syndrome in 2006. Our study revealed that DAC enhanced pyroptosis in CRC by demethylating GSDME, thereby reversing immunotherapy resistance induced by KIAA1199. This study introduces a novel clinical drug therapy combination, offering a promising avenue for exploring innovative therapeutic strategies to enhance immunotherapy efficacy in patients with CRC who are unresponsive to conventional immunotherapy approaches. Further clinical trials are warranted to validate the efficacy of DAC and other demethylating agents in reversing immunotherapy resistance in CRC.

Pyroptosis is known for its ability to recruit immune cells and modulate the immune microenvironment by releasing chemokines.^{9 60} Our previous investigations identified KIAA1199 as a factor that contributes to immunotherapy resistance by hindering CD8⁺ T cell infiltration.^{25 26} Here, we elucidated the role of KIAA1199 in inhibiting CD8⁺ T cell infiltration by suppressing pyroptosis and IL-1 β release. Furthermore, we found that DAC could recruit CD8⁺ T cells by inducing cell pyroptosis and subsequent IL-1 β release, thereby reversing immunotherapy resistance in CRC. These findings shed light on the potential mechanism by which pyroptosis activates the tumor immune microenvironment and further explore the downstream pathways through which DAC activates the immune microenvironment via pyroptosis, consequently reversing immunotherapy resistance.

CONCLUSIONS

In conclusion, our study elucidated the role of pyroptosis in shaping the response of patients with CRC to immunotherapy and elucidated the underlying mechanisms. We found that KIAA1199 inhibits pyroptosis via the DNMT1/GSDME pathway, consequently promoting resistance to immunotherapy (online supplemental figure 16). Additionally, we explored the clinical significance of pyroptosis-related genes and KIAA1199 as potential biomarkers for predicting immunotherapy responses and proposed a novel clinical treatment strategy involving the combination of DAC with ICIs. This approach aimed to reverse KIAA1199-mediated immunotherapy resistance by augmenting pyroptosis.

Our findings provide valuable insights for enhancing the efficacy of immunotherapy in patients with CRC who exhibit resistance to conventional immunotherapy approaches. In future studies, we plan to address the limitations of our current study design by using larger sample sizes to verify our pyroptosis models for predicting immunotherapy responses. Additionally, we will design and conduct a phase I clinical trial to evaluate the efficacy of decitabine in combination with ICIs, aiming to validate this method for reversing immunotherapy resistance in patients with CRC.

Author affiliations

¹Cancer Center, Union Hospital, Tongji Medical College, Huazhong University of Science and Technology, Wuhan, China

²Institute of Radiation Oncology, Union Hospital, Tongji Medical College, Huazhong University of Science and Technology, Wuhan, China

³Hubei Key Laboratory of Precision Radiation Oncology, Wuhan, China

⁴Department of Pathology, Union Hospital, Tongji Medical College, Huazhong University of Science and Technology, Wuhan, China

⁵Wuhan YZY Medical Science & Technology Co., Ltd, Wuhan, China

Acknowledgements The authors appreciate all the patients included in this study.

Contributors LSL, YHY, PYZ and JGZ conducted experiments. LSL and DJZ wrote the manuscript. LZ and DJZ designed research studies and analyzed data. DWZ, ZYL, DDY and JHR acquired data. PFZ and JZ provided reagents. LZ, DJZ and TZ supervised the project. TZ is the guarantor of the study.

Funding This work is supported by the National Natural Science Foundation of China (82272711 to DJZ, 82272900 to LZ, and 82373050 to TZ).

Competing interests No, there are no competing interests.

Patient consent for publication Written informed consent was obtained from the patient for publication of this case report and any accompanying images.

Ethics approval All animal experiments conducted in this study were approved by the Laboratory Animal Management and Use Committee of Hubei Provincial Center for Disease Control and Prevention (202410259). All human experiments conducted in this study were ethically approved by the Medical Ethics Committee of Tongji Medical College, Huazhong University of Science and Technology (UHCT20210271-01). Written informed consent was obtained before participation in the human studies.

Provenance and peer review Not commissioned; externally peer reviewed.

Data availability statement The data supporting the findings of this study are included in the article and supplementary materials. They are available from the corresponding authors (taozhangxh@hust.edu.cn and zhangdejun@hust.edu.cn) on reasonable request. The TCGA-COAD and TCGA-READ datasets can be accessed through the Genomic Data Commons Data Portal of the National Cancer Institute (<https://portal.gdc.cancer.gov/>).

Supplemental material This content has been supplied by the author(s). It has not been vetted by BMJ Publishing Group Limited (BMJ) and may not have been peer-reviewed. Any opinions or recommendations discussed are solely those of the author(s) and are not endorsed by BMJ. BMJ disclaims all liability and responsibility arising from any reliance placed on the content. Where the content includes any translated material, BMJ does not warrant the accuracy and reliability of the translations (including but not limited to local regulations, clinical guidelines, terminology, drug names and drug dosages), and is not responsible for any error and/or omissions arising from translation and adaptation or otherwise.

Open access This is an open access article distributed in accordance with the Creative Commons Attribution Non Commercial (CC BY-NC 4.0) license, which permits others to distribute, remix, adapt, build upon this work non-commercially, and license their derivative works on different terms, provided the original work is properly cited, appropriate credit is given, any changes made indicated, and the use is non-commercial. See <http://creativecommons.org/licenses/by-nc/4.0/>.

ORCID iD

Tao Zhang <http://orcid.org/0000-0003-4018-3393>

REFERENCES

- 1 Sung H, Ferlay J, Siegel RL, *et al.* Global Cancer Statistics 2020: GLOBOCAN Estimates of Incidence and Mortality Worldwide for 36 Cancers in 185 Countries. *CA Cancer J Clin* 2021;71:209–49.
- 2 Jin Z, Sinicrope FA. Mismatch Repair-Deficient Colorectal Cancer: Building on Checkpoint Blockade. *J Clin Oncol* 2022;40:2735–50.
- 3 Cercek A, Lumish M, Sinopoli J, *et al.* PD-1 Blockade in Mismatch Repair-Deficient, Locally Advanced Rectal Cancer. *N Engl J Med* 2022;386:2363–76.
- 4 Diaz LA Jr, Shiu K-K, Kim T-W, *et al.* Pembrolizumab versus chemotherapy for microsatellite instability-high or mismatch repair-deficient metastatic colorectal cancer (KEYNOTE-177): final analysis of a randomised, open-label, phase 3 study. *Lancet Oncol* 2022;23:659–70.
- 5 Zeng F-L, Chen J-F. Application of Immune Checkpoint Inhibitors in the Treatment of Cholangiocarcinoma. *Technol Cancer Res Treat* 2021;20:15330338211039952.
- 6 Yang L, Yang J, Kleppe A, *et al.* Personalizing adjuvant therapy for patients with colorectal cancer. *Nat Rev Clin Oncol* 2024;21:67–79.
- 7 Zhang Z, Zhang Y, Xia S, *et al.* Gasdermin E suppresses tumour growth by activating anti-tumour immunity. *Nature New Biol* 2020;579:415–20.
- 8 Barnett KC, Li S, Liang K, *et al.* A 360° view of the inflammasome: Mechanisms of activation, cell death, and diseases. *Cell* 2023;186:2288–312.
- 9 Li L, Jiang M, Qi L, *et al.* Pyroptosis, a new bridge to tumor immunity. *Cancer Sci* 2021;112:3979–94.
- 10 Erkes DA, Cai W, Sanchez IM, *et al.* Mutant BRAF and MEK Inhibitors Regulate the Tumor Immune Microenvironment via Pyroptosis. *Cancer Discov* 2020;10:254–69.
- 11 Hage C, Hoves S, Strauss L, *et al.* Sorafenib Induces Pyroptosis in Macrophages and Triggers Natural Killer Cell-Mediated Cytotoxicity Against Hepatocellular Carcinoma. *Hepatology* 2019;70:1280–97.
- 12 Wang Q, Wang Y, Ding J, *et al.* A bioorthogonal system reveals antitumour immune function of pyroptosis. *Nature New Biol* 2020;579:421–6.
- 13 Zhao P, Wang M, Chen M, *et al.* Programming cell pyroptosis with biomimetic nanoparticles for solid tumor immunotherapy. *Biomaterials* 2020;254.
- 14 Evensen NA, Kescu C, Nguyen H-L, *et al.* Unraveling the role of KIAA1199, a novel endoplasmic reticulum protein, in cancer cell migration. *J Natl Cancer Inst* 2013;105:1402–16.
- 15 Xie G, Dong P, Chen H, *et al.* Decreased expression of ATF3, orchestrated by β -catenin/TCF3, miR-17-5p and HOXA11-AS, promoted gastric cancer progression via increased β -catenin and CEMIP. *Exp Mol Med* 2021;53:1706–22.
- 16 Rodrigues G, Hoshino A, Kenific CM, *et al.* Tumour exosomal CEMIP protein promotes cancer cell colonization in brain metastasis. *Nat Cell Biol* 2019;21:1403–12.
- 17 Tang Z, Ding Y, Shen Q, *et al.* KIAA1199 promotes invasion and migration in non-small-cell lung cancer (NSCLC) via PI3K-Akt mediated EMT. *J Mol Med (Berl)* 2019;97:127–40.
- 18 Yu Y, Liu B, Li X, *et al.* ATF4/CEMIP/PKC α promotes anoikis resistance by enhancing protective autophagy in prostate cancer cells. *Cell Death Dis* 2022;13:46.
- 19 Xu Y, Xu H, Li M, *et al.* KIAA1199 promotes sorafenib tolerance and the metastasis of hepatocellular carcinoma by activating the EGF/EGFR-dependent epithelial-mesenchymal transition program. *Cancer Lett* 2019;454:78–89.
- 20 Jiao X, Ye J, Wang X, *et al.* KIAA1199, a Target of MicoRNA-486-5p, Promotes Papillary Thyroid Cancer Invasion by Influencing Epithelial-Mesenchymal Transition (EMT). *Med Sci Monit* 2019;25:6788–96.
- 21 Zhang D, Zhao L, Shen Q, *et al.* Down-regulation of KIAA1199/CEMIP by miR-216a suppresses tumor invasion and metastasis in colorectal cancer. *Int J Cancer* 2017;140:2298–309.
- 22 Zhao L, Zhang D, Shen Q, *et al.* KIAA1199 promotes metastasis of colorectal cancer cells via microtubule destabilization regulated by a PP2A/stathmin pathway. *Oncogene* 2019;38:935–49.
- 23 Hua Q, Zhang B, Xu G, *et al.* CEMIP, a novel adaptor protein of OGT, promotes colorectal cancer metastasis through glutamine metabolic reprogramming via reciprocal regulation of β -catenin. *Oncogene* 2021;40:6443–55.
- 24 Xu G, Zhao L, Hua Q, *et al.* CEMIP, acting as a scaffold protein for bridging GRAF1 and MIB1, promotes colorectal cancer metastasis via activating CDC42/MAPK pathway. *Cell Death Dis* 2023;14:167.
- 25 Wang H, Zhang B, Li R, *et al.* KIAA1199 drives immune suppression to promote colorectal cancer liver metastasis by modulating neutrophil infiltration. *Hepatology* 2022;76:967–81.
- 26 Zhang B, Li J, Hua Q, *et al.* Tumor CEMIP drives immune evasion of colorectal cancer via MHC-I internalization and degradation. *J Immunother Cancer* 2023;11:e005592.
- 27 Li T, Fu J, Zeng Z, *et al.* TIMER2.0 for analysis of tumor-infiltrating immune cells. *Nucleic Acids Res* 2020;48:W509–14.
- 28 Subramanian A, Tamayo P, Mootha VK, *et al.* Gene set enrichment analysis: A knowledge-based approach for interpreting genome-wide expression profiles. *Proc Natl Acad Sci USA* 2005;102:15545–50.
- 29 Van Allen EM, Miao D, Schilling B, *et al.* Genomic correlates of response to CTLA-4 blockade in metastatic melanoma. *Science* 2015;350:207–11.
- 30 Hugo W, Zaretsky JM, Sun L, *et al.* Genomic and Transcriptomic Features of Response to Anti-PD-1 Therapy in Metastatic Melanoma. *Cell* 2017;168:542.
- 31 Biller LH, Schrag D. Diagnosis and Treatment of Metastatic Colorectal Cancer: A Review. *JAMA* 2021;325:669–85.
- 32 Wang Y, Gao W, Shi X, *et al.* Chemotherapy drugs induce pyroptosis through caspase-3 cleavage of a gasdermin. *Nature New Biol* 2017;547:99–103.
- 33 Shi J, Zhao Y, Wang K, *et al.* Cleavage of GSDMD by inflammatory caspases determines pyroptotic cell death. *Nature New Biol* 2015;526:660–5.
- 34 Hua Q, Lu Y, Wang D, *et al.* KIAA1199 promotes oxaliplatin resistance and epithelial mesenchymal transition of colorectal cancer via protein O-GlcNAcylation. *Transl Oncol* 2023;28:101617.
- 35 Wang A, Zhu J, Li J, *et al.* Downregulation of KIAA1199 by miR-486-5p suppresses tumorigenesis in lung cancer. *Cancer Med* 2020;9:5570–86.
- 36 Galluzzi L, Buqué A, Kepp O, *et al.* Immunogenic cell death in cancer and infectious disease. *Nat Rev Immunol* 2017;17:97–111.
- 37 Dong S, Shi Y, Dong X, *et al.* Gasdermin E is required for induction of pyroptosis and severe disease during enterovirus 71 infection. *J Biol Chem* 2022;298:101850.
- 38 Lyko F. The DNA methyltransferase family: a versatile toolkit for epigenetic regulation. *Nat Rev Genet* 2018;19:81–92.
- 39 Hu J, Dong Y, Ding L, *et al.* Local delivery of arsenic trioxide nanoparticles for hepatocellular carcinoma treatment. *Signal Transduct Target Ther* 2019;4:28.
- 40 Tian A, Wu T, Zhang Y, *et al.* Triggering pyroptosis enhances the antitumor efficacy of PARP inhibitors in prostate cancer. *Cell Oncol (Dordr)* 2023;46:1855–70.
- 41 Yu X, Xing G, Sheng S, *et al.* Neutrophil Camouflaged Stealth Nanovehicle for Photothermal-Induced Tumor Immunotherapy by Triggering Pyroptosis. *Adv Sci (Weinh)* 2023;10.
- 42 Zhang Q, Shi D, Guo M, *et al.* Radiofrequency-Activated Pyroptosis of Bi-Valent Gold Nanocluster for Cancer Immunotherapy. *ACS Nano* 2023;17:515–29.
- 43 Hu J, You Y, Zhu L, *et al.* Sialic Acid-Functionalized Pyroptosis Nanotuner for Epigenetic Regulation and Enhanced Cancer Immunotherapy. *Small* 2024;20:e2306905.
- 44 Sun S, He Y, Xu J, *et al.* Enhancing cell pyroptosis with biomimetic nanoparticles for melanoma chemo-immunotherapy. *J Control Release* 2024;367:470–85.
- 45 Xie B, Liu T, Chen S, *et al.* Combination of DNA demethylation and chemotherapy to trigger cell pyroptosis for inhalation treatment of lung cancer. *Nanoscale* 2021;13:18608–15.
- 46 Smalley KSM. Two Worlds Collide: Unraveling the Role of the Immune System in BRAF-MEK Inhibitor Responses. *Cancer Discov* 2020;10:176–8.
- 47 Wang Q, Liu P, Wen Y, *et al.* Metal-enriched HSP90 nanoinhibitor overcomes heat resistance in hyperthermic intraperitoneal chemotherapy used for peritoneal metastases. *Mol Cancer* 2023;22:95.
- 48 Su W, Qiu W, Li S, *et al.* A Dual-Responsive STAT3 Inhibitor Nanoprodug Combined with Oncolytic Virus Elicits Synergistic Antitumor Immune Responses by Igniting Pyroptosis. *Adv Mater Weinheim* 2023;35.
- 49 Liu Z, Li X, Gao Y, *et al.* Epigenetic reprogramming of Runx3 reinforces CD8⁺ T-cell function and improves the clinical response to immunotherapy. *Mol Cancer* 2023;22:84.
- 50 Loo Yau H, Bell E, Ettayebi I, *et al.* DNA hypomethylating agents increase activation and cytolytic activity of CD8⁺ T cells. *Mol Cell* 2021;81:1469–83.
- 51 Xia S, Zhang Z, Magupalli VG, *et al.* Gasdermin D pore structure reveals preferential release of mature interleukin-1. *Nature New Biol* 2021;593:607–11.
- 52 Liu M, Li Q, Liang Y. Pyroptosis-related genes prognostic model for predicting targeted therapy and immunotherapy response in soft tissue sarcoma. *Front Pharmacol* 2023;14:1188473.
- 53 Qi X, Che X, Li Q, *et al.* Potential Application of Pyroptosis in Kidney Renal Clear Cell Carcinoma Immunotherapy and Targeted Therapy. *Front Pharmacol* 2022;13:918647.

- 54 Gong Z, Li Q, Yang J, *et al.* Identification of a Pyroptosis-Related Gene Signature for Predicting the Immune Status and Prognosis in Lung Adenocarcinoma. *Front Bioeng Biotechnol* 2022;10:852734.
- 55 Xie R, Xie M, Zhu L, *et al.* The Relationship of Pyroptosis-Related Genes, Patient Outcomes, and Tumor-Infiltrating Cells in Bladder Urothelial Carcinoma (BLCA). *Front Pharmacol* 2022;13:930951.
- 56 Ma S, Wang F, Wang N, *et al.* Extended Application of Genomic Selection to Screen Multi-Omics Data for the Development of Novel Pyroptosis-Immune Signatures and Predicting Immunotherapy of Glioma. *Front Pharmacol* 2022;13:893160.
- 57 Zheng Y, Huang C, Lu L, *et al.* STOML2 potentiates metastasis of hepatocellular carcinoma by promoting PINK1-mediated mitophagy and regulates sensitivity to lenvatinib. *J Hematol Oncol* 2021;14:16.
- 58 Kim MS, Chang X, Yamashita K, *et al.* Aberrant promoter methylation and tumor suppressive activity of the DFNA5 gene in colorectal carcinoma. *Oncogene* 2008;27:3624–34.
- 59 Yokomizo K, Harada Y, Kijima K, *et al.* Methylation of the DFNA5 gene is frequently detected in colorectal cancer. *Anticancer Res* 2012;32:1319–22.
- 60 Rosenbaum SR, Wilski NA, Aplin AE. Fueling the Fire: Inflammatory Forms of Cell Death and Implications for Cancer Immunotherapy. *Cancer Discov* 2021;11:266–81.